이학석사 학위논문

Vps13b 유전자 적중 생쥐의 불안 행동과 일부 인지 기능에 대한 연구

Studies on anxiety-like behavior and cognitive functions in *Vps13b* knockout mice

2018년 2월

서울대학교 대학원

생명과학부

이 로 운

Vps13b 유전자 적중 생쥐의 불안 행동과 일부 인지 기능에 대한 연구

Studies on anxiety-like behavior and cognitive functions in *Vps13b* knockout mice

지도교수 강 봉 균

이 논문을 이학석사 학위논문으로 제출함

2017년 12월

서울대학교 대학원

생명과학부

이 로 운

이 로 운의 이학석사 학위논문을 인준함

2017년 12월

위 원 장 _____ (인)

부위원장 _____ (인)

위 원 _____ (인)

Studies on anxiety-like behavior and cognitive functions in *Vps13b* knockout mice

Advisor. Professor Bong-Kiun Kaang

A dissertation submitted to the Graduate Faculty of Seoul National University in partial fulfillment of the requirement for the Degree of Master of Science

Ro Un Lee

Graduate School of Natural Sciences

Seoul National University

Biological Sciences Major

Table of Contents

Page

List of Figures 2

Abstract 3

Introduction 5

Materials and Methods 8

Results 14

Figures 19

Discussion 39

References 42

Abstract in Korean 50

List of Figures

Page

Figure 1. Characterization of *Vps13b* KO mice. 19

Figure 2. Overview of behavioral scheme of *Vps13b* KO mice. 21

Figure 3. *Vps13b* KO mice show hypoactivtity in an open field test, but anxiety−like behavior was normal. 22

Figure 4. *Vps13b* KO mice show normal anxiety−like behavior in an elevated zero maze test but tendency of anxious in a light−dark box test. 24

Figure 5. *Vps13b* KO mice exhibit normal working memory in the Y−maze test. 26

Figure 6. *Vps13b* KO mice have normal fear memory in the contextual fear conditioning. 28

Figure 7. *Vps13b* KO mice show impaired spatial learning and memory in the Morris water maze. 30

Figure 8. *Vps13b* KO mice show normal social interaction in three−chamber assays. 36

Abstract

Studies on anxiety-like behavior and cognitive functions in Vps13b knockout mice

Ro Un Lee

Department of Biological Sciences

The Graduate School

Seoul National University

Vacuolar protein sorting-associated protein 13B (VPS13B), also known as COH1, is one of the VPS13 family members which cause distinct neurodegenerative and developmental disorders, and involved in transmembrane transport, Golgi integrity, and neuritogenesis. There are many human studies revealing patients with Cohen syndrome (CS) have a mutation in *VPS13B* gene. A mutation in *VPS13B* gene is also associated with autism spectrum disorder (ASD). However, pathogenesis of CS is not yet defined clearly. Here, I examined behavioral aspects of *Vps13b* knockout (KO)

mice as a CS mouse model. I found that *Vps13b* KO mice exhibited hypoactivity and impaired spatial learning and memory, compared to wild-type (WT) mice littermates. However, *Vps13b* KO mice showed normal anxiety-like phenotypes, working memory, fear memory, and social behavior. This study reveals behavioral phenotypes of *Vps13b* KO mice for the first time.

Keyword : Cohen syndrome, *Vps13b* knockout mice, behavioral study, hypoactivity, spatial learning and memory

Student Number : 2016-20393

Introduction

VPS13B (also known as COH1) is one of the VPS13 protein family members which consist of four mammalian members; VPS13A, VPS13B, VPS13C, and VPS13D. Each of *VPS13* gene members, except *VPS13D*, is related to certain human neurological disorders, such as chorea acanthocytosis and Parkinson's disease (Rampoldi et al., 2001; Ueno et al., 2001; Lesage et al., 2016). Among these members, mutations in the *VPS13B* gene have been identified mainly in individuals with recessive disorder Cohen syndrome (CS) (Balikova et al., 2009). Clinical features of CS patients involve microcephaly, intellectual disability, hypotonia, developmental delay, and many more (El Chehadeh et al., 2010; El Chehadeh et al., 2012). In addition, *VPS13B* mutations have been found in patients with autism spectrum disorder (ASD), which is one of well-known neurodevelopmental disorders characterized by impaired social interaction, deficit in social communication, and restricted and repetitive behaviors (Yu et al., 2013; Murphy et al., 2016).

VPS13B is located on chromosome 8q22, and spans 864kb of genomic DNA sequences with 62 exons encoding a putative transmembrane protein of 4,022 amino acids (Kolehmainen et al., 2003; Velayos-Baeza et al., 2004). Furthermore, *VPS13B* gene has

several functional roles in cells, such as Golgi complex integrity, neuronal outgrowth, regulator of adipogenesis, and glycosylation (Seifert et al., 2011; Seifert et al., 2015; Kolehmainen et al., 2003; Limoge et al., 2015; Duplomb et al., 2014). However, it is still not well defined how loss or mutation of *VPS13B* gene lead to neurological phenotypes of CS. Therefore, it is necessary to investigate and discover more about the underlying mechanisms and roles of the gene.

Since CS is very rare and the number of cases is limited, it is challenging to study the molecular pathogenesis using human specimen. In order to overcome this problem, mouse model system, which has many features in common with human, has been widely used and favored for studying human diseases (Kaczmarczyk et al., 2015; Houtkooper et al., 2011). For example, Clustered Regularly Interspaced Short Palindromic Repeats/CRISPR-associated 9 (CRISPR/Cas9) system provides a genome-editing and genome targeting tool, allowing researchers to manipulate specific genomic element (Jinek et al., 2012; Cho et al., 2013). Among VPS13 family members, *Vps13A* is the only gene that successfully established animal model for chorea acanthocytosis (Sakimoto et al., 2016; Vonk et al., 2017).

In this study, I performed a variety of behavioral tasks to investigate behavioral phenotypes of *Vps13b* KO mice, which carry a

deletion of exon 2 of the *Vps13b* gene. This report provides the first insight into the behavioral phenotypes of *Vps13b* KO mice as a model of human CS.

Materials and methods

Mice

Mice were generated and obtained from Macrogen. Mice were designed to have 156 base pairs (bp) deletion in their exon 2, using CRISPR/Cas9 system. Genotypes of mice were determined by PCR using primers shown in Table 1. DNA from mouse tail was prepared by incubation at 60℃ overnight with a mixture of DirectPCR Lysis Reagen (Viagen) and Proteinase K (Thermo Fisher). Polymerase chain reaction (PCR) mixture of Han taq (Genenmed), Han taq buffer (Genenmed), forward/reverse primers, deoxynucleoside triphosphate (Roche) and distilled water was added to the DNA extract. PCR cycling conditions were 98℃ for 3 min, followed by 35 cycles of 95℃ for 30 s, 60℃ for 30 s, 72℃ for 1 min, followed by 72℃ for 5 min. The PCR products were visualized by staining with ethidium bromide in a 2% agarose gel. For behavioral testing, adult mice (8–19 weeks at the start of experiments) were used. Mice were exposed to 12h light/dark cycles and provided with access to food and water *ad libitum*. All experimental protocols were approved by the Institutional Animal Care and Use Committee of Seoul National University.

Quantitative real-time PCR (qRT-PCR)

Total RNA was isolated from the brain tissues of WT and KO mice using TRIzol (Invitrogen). RNA was reverse-transcribed using SuperScript Ⅲ and random hexamers (Invitrogen). Amplification was performed using 7300 real-time PCR System (Applied Biosystems) in the presence of SYBR premix ExTaqⅡ (RR820A, Takara). Cycling conditions were 95℃ for 30s, followed by 40 cycles of 95℃ for 5s and 60℃ for 31s. qRT-PCR data were normalized for GAPDH mRNAs to control the variation, and individual data sets were normalized to the WT samples. Representative experiment performed in triplicate. n=3(WT), 2(HT), 4(KO).

Table 1. Primers for PCR and qRT-PCR

Primer	Primer sequence(5′ to 3′)
Oligonucleotide for genotyping (amplicon size: 514 bp)	F GCC AAG CTT CCT GAG AAG TG R GTG CTT GAG AAC TGA GTA
GAPDH	F GGA GCG AGA TCC CTC CAA AAT R GGC TGT TGT CAT ACT TCT CAT GG
Exon 2,3 spanning	F CGA GTT AAA GTT GGA CGT TCT GG R AGG TTC GGA GCC CAA TTT TGT

Behavioral experiments

Prior to all behavioral tests, mice were allowed to acclimate to the test room for at least 30 min. After each test, the apparatus was cleaned with 70% alcohol and distilled water and allowed to dry enough before testing the next mice.

Open field test. Mice were placed in the center of open field (40 x 40 x 40 cm) under dim light, and allowed to move freely for 30 min. The movement was analyzed by tracking program, EthoVision 3.1, Nodulus.

Elevated zero maze. The maze (round-shaped, 50 cm diameter, 5 cm width) was consisted of two close arms and two open arms, elevated to a height of 65cm above the floor. Mice were first placed in the center of closed arm, and allowed to move both arms freely for 10 min under bright light. The time spent in each arms was analyzed by EthoVision 3.1, Nodulus.

Light dark box test. Light dark box apparatus was consisted of light and dark chambers adhered to each other with a gate in between two chambers. The illumination of light chamber (20 x 30 x 20 cm, a large

compartment) was 404–408 lux and that of dark chamber (20 x 13 x 20 cm, a small apartment) was ~3 lux. Mice were first introduced to the dark chamber, in which was then enclosed with a lid. Mice were allowed to move freely between two chambers for 10 min. The time spent in each chamber was manually and blindly counted.

Y–maze test. Mice were introduced to the center of the Y–maze with three identical arms at a 120 ° angle from each other, and allowed to move freely for 8 min under dim light. Each arm was 30 cm long, 6 cm wide, and 15 cm height. The sequence of entries and the total number of each arm entries were recorded, and manually and blindly counted.

Contextual fear conditioning. Mice were handled to the experimenter and surroundings for 3 min for 3–consecutive days. For conditioning test, mice were put into conditioned chamber (Coulbourn Instruments) for 3 min, and an electrical foot shock (3s duration, 0.8mA intensity) was presented through the floor grid. Immediately after the conditioning, mice were returned to the home cages. For fear memory test, mice were exposed to the same context for 3 min, but no shock was given. Freezing level was automatically quantified by Freeze Frame software.

Morris water maze. Mice were handled for 3 min for 5-consecutive days. For training, mice were put into a white opaque water-filled tank (140 cm diameter, 100 cm height), that was placed in a test room with multiple spatial cues around. Mice were released at the edge of the maze, and allowed to find the hidden platform (round-shaped, 10 cm diameter), which was placed at the center of a target quadrant (TQ), within 60 s. If they were unable to find the platform, they were guided until they could find their ways to the platform. Mice were trained with 4 trials per day. Probe tests were conducted at day 7 and 11 in the same condition, but in the absence of platform. Training was not performed after the probe tests considering tiredness of mice. The tank was divided into four different quadrants, and water temperature was optimized to 21-22℃. The time spent in each quadrant, the number of platform crossings, distance moved from platform, and mean velocity were evaluated by EthoVision 3.1, Nodulus.

For visual platform task using the Morris water maze, a visible black flag was placed on the platform. Mice were allowed to swim toward the target, and escape latency was measured using EthoVision 3.1, Nodulus.

Three chamber test. Chamber apparatus was separated into three different areas next to each other by dividers. Test and stranger mice

were separately habituated in the empty chambers or wired-cups, respectively, for 3-consecutive days. For sociability test, stranger 1 and object were placed in each wired-cup. Dividers were removed, and test mice were introduced into the neutral chamber and allowed to explore the chamber for 10 min. For social novelty test, object was replaced with stranger 2, and test mice were introduced and allowed to explore between stranger 1 and 2. The time spent exploring object, stranger 1, or stranger 2 was manually and blindly counted.

Statistical analysis

All experimental data were analyzed using Graphpad Prism 5 software. Statistical comparisons were made using unpaired *t*-test, one-way ANOVA, and two-way ANOVA. Further comparison was performed by the post hoc Bonferroni test. In all cases, statistical significance was represented by $*p < 0.05$, $**p < 0.01$ and $***p < 0.001$. All data shown are mean±SEM.

Results

Generation and characterization of *Vps13b* KO mice.

Homozygous *Vps13b* KO mice were generated by deleting 156 bp in exon 2 of *Vps13b* gene (Fig. 1A). To verify the deletion in *Vps13b* mice, I used various PCR methods. I used primer pairs spanning exon 2, 3 to detect endogenous mRNA levels in mice. I confirmed that homozygous *Vps13b* KO mice did not show mRNA expression, whereas heterozygous mutant mice expressed approximately 50% of *Vps13b* mRNA level (Fig. 1B). Genotypes of mice were determined by genomic PCR, which showed 145 bp band size in WT mice and 135 bp KO mice as expected (Fig. 1C).

Vps13b KO mice showed hypoactivity.

Anxiety-like behaviors of *Vps13b* mice were examined through various behavioral tasks. First, I conducted open field test (Fig. 3A). Mice typically spend a greater amount of time exploring the peripheral zone than the center zone. As expected, mice spent most of their time in the periphery of the arena and the least in the 10 cm

center zone. The time spent in each zone showed no difference between KO and WT groups (Fig. 3B). Furthermore, locomotor activity was measured based on the distance moved over time. The distance moved and mean velocity in the open field were significantly reduced in KO mice, suggesting hypoactivity of KO mice (Fig. 3C, 3D, 3D). Next, I performed other anxiety-like behavior tasks, elevated zero maze (EZM) test and light dark box test (LDT) (Fig. 4A, 4C). Mice naturally spend more time in closed arms in EZM, and prefer to move around the dark areas in the LDT. Both KO and WT mice spent more time in the closed arms than the open arms (Fig. 4B). In addition, although it was not statistically significant, KO mice showed a tendency to spend less time in lit areas in the LDT (Fig. 4D). Taken together, I conclude that KO mice showed normal basal anxiety levels, but were hypoactive.

Vps13b KO mice showed normal working and fear memories.

Previous studies on other Vps families, like Vps10, showed impaired memory performances in *Vps* KO mice (Knight et al., 2016). Thus, *Vps13b* KO mice were also tested for working memory, using Y-maze task (Fig. 5A). Normal mice prefer to visit a new arm of the maze and show high rate of alternation. The percentage of alternation

of KO mice did not differ from that of WT mice (Fig. 5B). Although the total number of entries seemed to have a decreasing pattern in KO mice, there was no significant difference, compared to WT mice (Fig. 5C). Next, the contextual fear conditioning paradigm was performed to examine hippocampus-dependent associative fear memory in KO mice (Fig. 6A). In pre-training test, mice were given a mild foot shock, and then on the next day, they were tested whether they could show distinct fear memory when re-exposed to the same context. Both groups showed similar freezing levels during training (Fig. 6B). In retrieval test 1, similar level of freezing was induced in both WT and KO mice (Fig. 6B). To examine whether the remote fear memory is altered in *Vps13b* KO mice, I carried out retrieval test again after 4 weeks. However, there was no difference between both groups and freezing levels were not much different from that observed in retrieval test 1. (Fig. 6B). Overall, KO mice had normal working and fear memories.

Vps13b KO mice showed abnormal hippocampus-dependent spatial learning and memory.

In order to assess hippocampus-dependent spatial learning and memory, I conducted the Morris water maze test. In this task, mice

were trained to use spatial cues around the maze to find an escape platform, which was hidden below the water maze, for several days. Then the platform was removed, and probe tests were performed at day 7 and 11 to assess memory of mice and ability to use spatial cues (Fig. 7A). I observed that escape latency of WT mice kept shortening, whereas that of KO mice seemed to unchanged over the training days (Fig. 7B). In probe test 1 at day 7, WT mice spent significantly longer time at TQ, in which the hidden platform was located. In case of KO mice, they showed no specific preference to any quadrants (Fig. 7C). The number of platform crossing times, the distance travelled from platform, and speed were not different between KO and WT groups (Fig. 7D, 7E, 7F). In probe test 2 at day 11, the result was the same as seen in probe test 1 (Fig. 7G, 7H, 7I, 7J). Therefore, KO mice exhibited impaired spatial learning and memory. I also tested whether the impaired phenotype was affected by visual abnormality in KO mice. A visual flag was placed on the platform allowing mice to see it very clearly (Fig. 7K). As a result, all mice managed to escape within 15 s, and therefore KO mice seemed to have normal visions (Fig. 7L).

Vps13b KO mice showed normal sociability.

As mentioned previously, autism patient also shows a mutation in

VPS13B gene (Yu et al., 2013). Therefore, I examined abnormalities in social interaction, which is one of the key characterizations of autism, using three-chamber test. Novel preference and social novelty recognition were performed to test the mice interacting with object or stranger mice 1 (stranger 1) and stranger 1 or stranger mice 2 (stranger 2) respectively (Fig. 8A), and then sociability index and social novelty index were calculated based on the interaction times to measure sociability. For both sociability index and social novelty index, KO and WT mice showed no difference (Fig. 8B). Thus, I conclude that KO mice did not show abnormalities in social interaction.

Figures

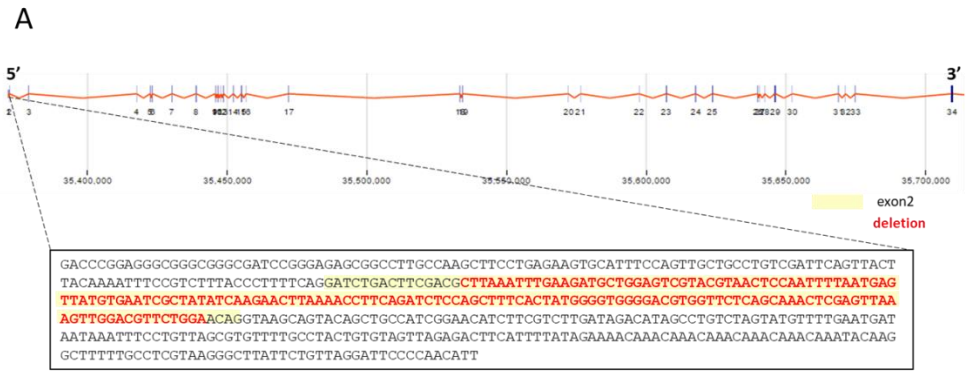
A
5′
3′
35,400,000
35,450,000
35,500,000
35,600,000
35,650,000
35,700,000
exon2
deletion
GACCCGGAGGGCGGGCGGGCGATCCGGGAGAGCGGCCTTGCCAAGCTTCCTGAGAAGTGCATTTCCAGTTGCTGCCTGTCGATTCAGTTACT
TACAAAATTTCCGTCTTTACCCTTTTCAGGATCTGACTTCGACGCTTAAATTTGAAGATGCTGGAGTCGTACGTAACTCCAATTTTAATGAG
TTATGTGAATCGCTATATCAAGAACTTAAAACCTTCAGATCTCCAGCTTTCACTATGGGGTGGGGACGTGGTTCTCAGCAAACTCGAGTTAA
AGTTGGACGTTCTGGAACAGGTAAGCAGTACAGCTGCCATCGGAACATCTTCGTCTTGATAGACATAGCCTGTCTAGTATGTTTTGAATGAT
AATAAATTTCCTGTTAGCGTGTTTTGCCTACTGTGTAGTTAGAGACTTCATTTTATAGAAAACAAACAAACAAACAAACAAATACAAG
GCTTTTTGCCTCGTAAGGGCTTATTCTGTTAGGATTCCCCAACATT
B
RNA level
(Normalized to GAPDH & Vps13b+/+)
1.5
1.0
0.5
0.0
n.d
Vps13b+/+
Vps13b+/-
Vps13b-/-
C
(bp)
+/-
+/+
-/-
600
500
400
300

Figure 1. Characterization of *Vps13b* KO mice.

(A) Targeted deletion of the *Vps13b* gene. Yellow highlight represents sequence of exon 2. Red-colored bold represents location of deletion. (B) Measurement of *Vps13b* RNA level using primers spanning exon 2, 3 (*Vps13b*$^{+/+}$: n=2; *Vps13b*$^{+/-}$: n=3; *Vps13b*$^{-/-}$: n.d, not detectable, n=3). (C) Genotypes of *Vps13b* mice (upper band size 514 bp; lower band size 358 bp).

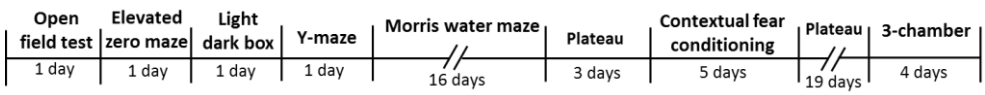

Figure 2. Overview of behavioral scheme of *Vps13b* KO mice.

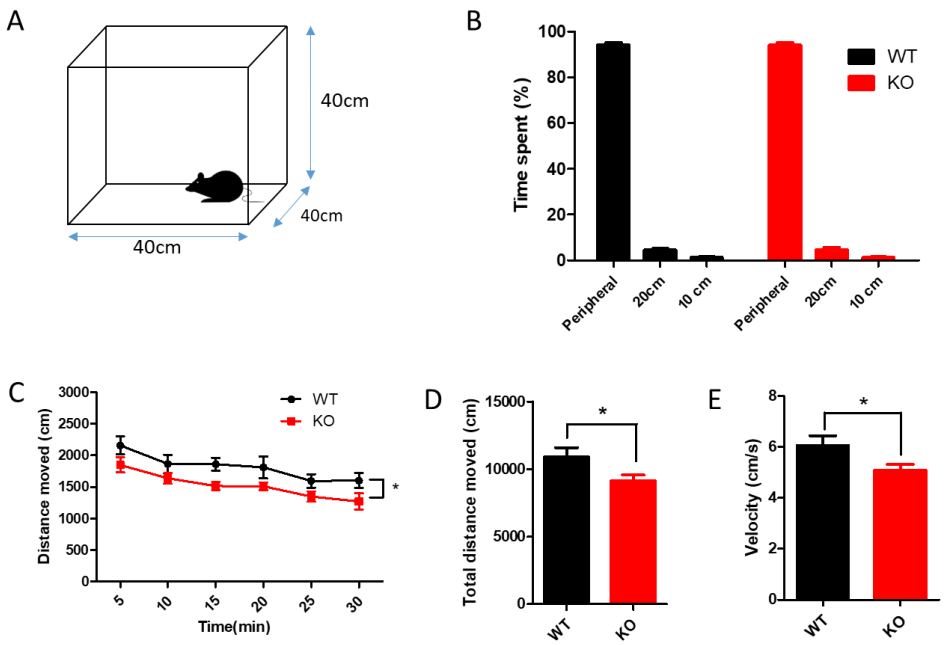
A
40cm
40cm
40cm
B
Time spent (%)
100
80
60
40
20
0
WT
KO
Peripheral
20cm
10 cm
Peripheral
20cm
10 cm
C
Distance moved (cm)
3000
2500
2000
1500
1000
500
0
WT
KO
*
5
10
15
20
25
30
Time(min)
D
Total distance moved (cm)
15000
10000
5000
0
*
WT
KO
E
Velocity (cm/s)
8
6
4
2
0
*
WT
KO

Figure 3. *Vps13b KO* mice show hypoactivity in an open field test, but anxiety-like behavior was normal.

(A) An open field apparatus. **(B)** Time spent in peripheral (40cm), 20cm, 10cm zones (WT: n=9; KO: n=12; two-way ANOVA, genotype x zone, $F_{2,38}$=0.01, p=0.9901; effect of genotype, $F_{1,38}$=0.23, p=0.6387; effect of zone, $F_{2,38}$=5790.45, p < 0.0001). **(C)** Distance moved measured in 5-min intervals across the 30-min test session (WT: n=9; KO: n=12; two-way ANOVA, genotype x time, $F_{5,95}$=0.23, p=0.9481; effect of genotype, $F_{1,95}$=5.04, p=0.0369; effect of time, $F_{5,95}$=18.30, p < 0.0001). **(D)** Total distance moved in cm (WT: 10940±685.0, n=9; KO: 9083±452.4, n=12; unpaired *t*-test, *p < 0.05). **(E)** Mean velocity (WT: 6.059±0.3852, n=9; KO: 5.081±0.2442; unpaired *t*-test, *p < 0.05). *p < 0.05, **p < 0.01 and ***p < 0.001. All data shown are mean±SEM.

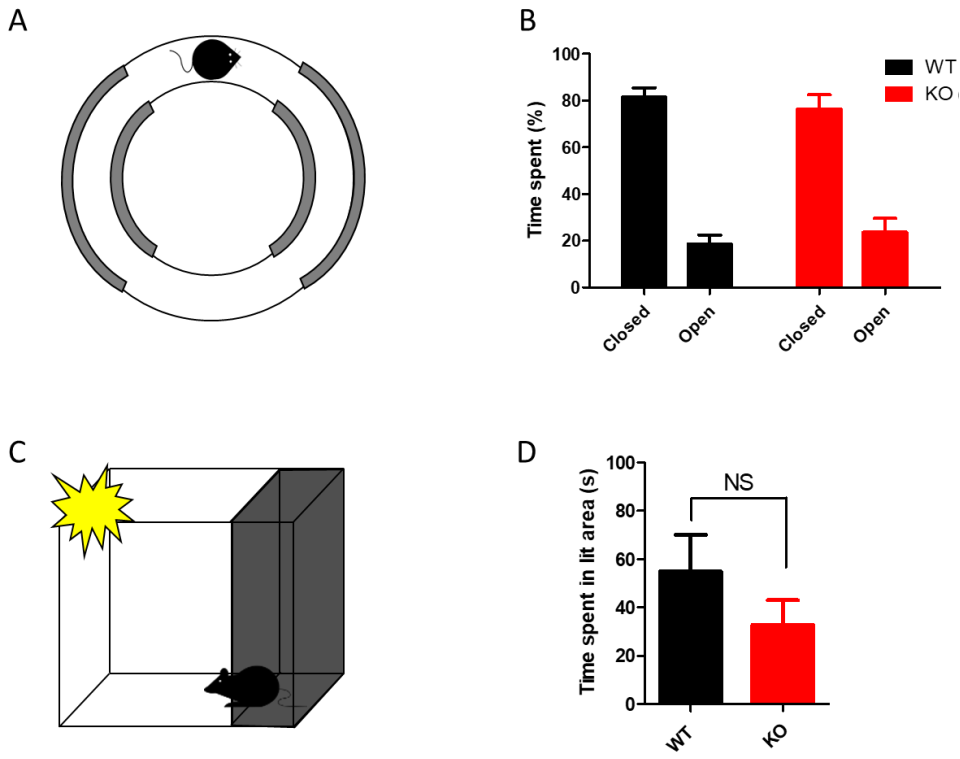
A
B
100
80
60
40
20
0
Time spent (%)
WT
KO
Closed
Open
Closed
Open
C
D
NS
Time spent in lit area (s)
100
80
60
40
20
0
WT
KO

Figure 4. *Vps13b* KO mice show normal anxiety-like behavior in an elevated zero maze but tendency of anxious in a light-dark box test.

(A) Elevated zero maze. (B) Time spent in closed and open arms (WT: n=9; KO: n=12; two-way ANOVA, genotype x sector, $F_{1,19}$=0.42, p=0.5242; effect of genotype, $F_{1,19}$=1.86, p=0.1889; effect of sector, $F_{1,19}$= 54.49, p < 0.0001). (C) Light dark box test apparatus. (D) Time spent in lit area (WT: 54.98±15.04, n=9; KO: 32.79±10.29, n=12; unpaired *t*-test, p=0.2225). All data shown are mean±SEM.

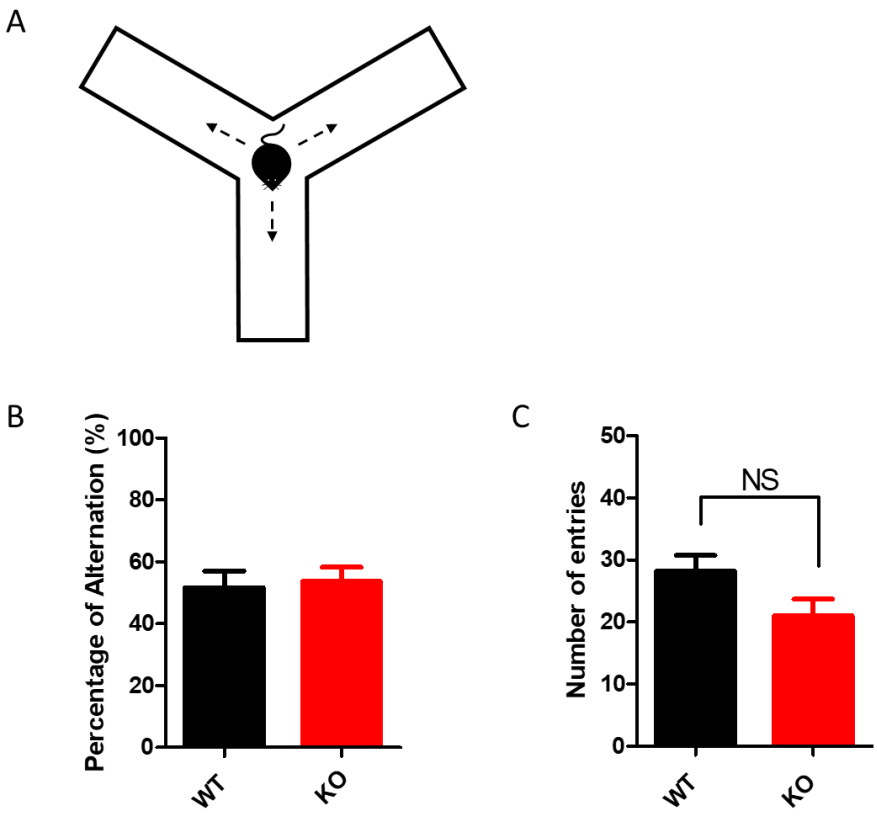
A
B
Percentage of Alternation (%)
100
80
60
40
20
0
WT
KO
C
Number of entries
50
40
30
20
10
0
NS
WT
KO

Figure 5. *Vps13b* KO mice exhibit normal working memory in the Y-maze test.

(A) Y-maze apparatus. (B) Alternation %(WT: 51.67±5.401, n=9; KO: 53.59±4.655, n=12; unpaired *t*-test, p=0.7901). (C) Number of entries (WT: 28.22±2.515, n=9; KO: 21.00±2.680, n=12; unpaired *t*-test, NS p=0.0719). NS: not significant. All data shown are mean±SEM.

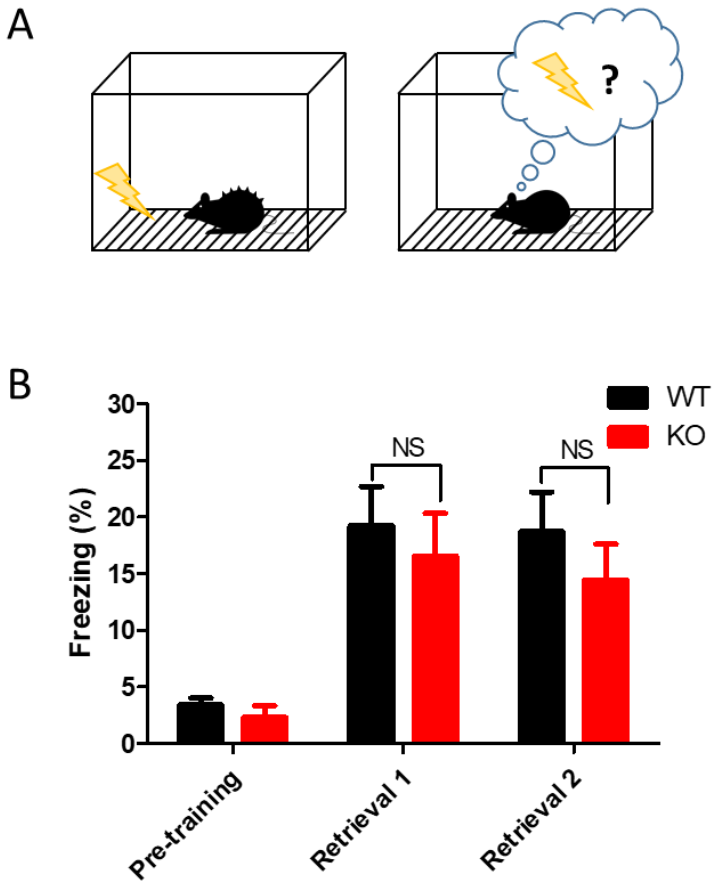
A
?
B
WT
KO
Freezing (%)
30
25
20
15
10
5
0
NS
NS
Pre-training
Retrieval 1
Retrieval 2

Figure 6. *Vps13b* KO mice exhibit normal contextual fear memory.

(A) Contextual fear conditioning paradigm. (B) Freezing levels in pre-training test, retrieval 1, and retrieval 2 (WT: n=9, KO: n=11; two-way ANOVA, genotype x condition, $F_{2,54}$=0.15, p=0.8616; effect of genotype, $F_{1,54}$ = 1.27, p=0.2647; effect of condition, $F_{2,54}$=16.31, p < 0.0001; Bonferroni posttests, NS: not significant). All data shown are mean±SEM.

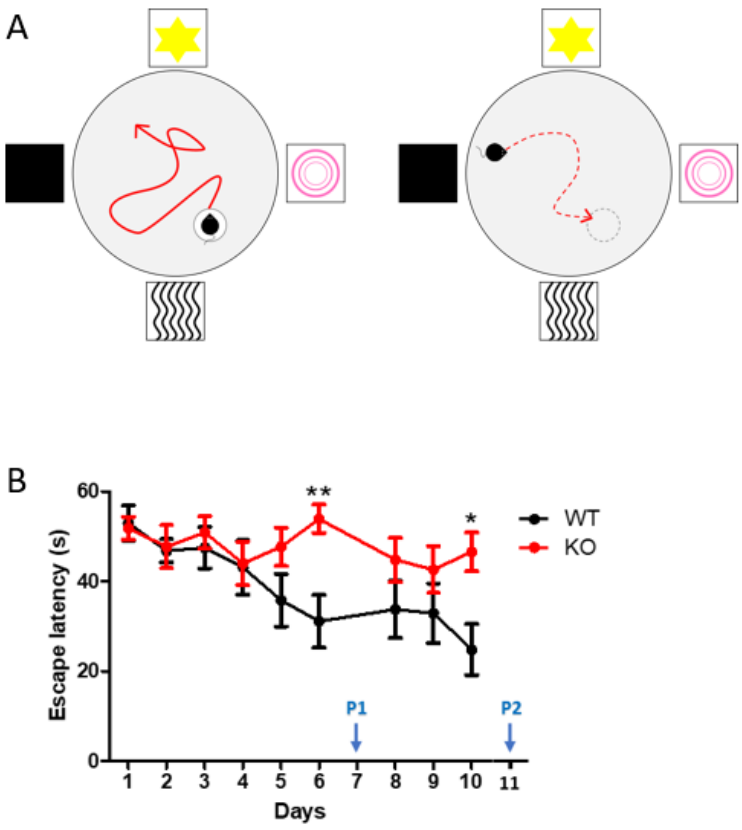
A
B
Escape latency (s)
60
40
20
0
**
*
WT
KO
P1
P2
1
2
3
4
5
6
7
8
9
10
11
Days

Probe test 1 at day 7

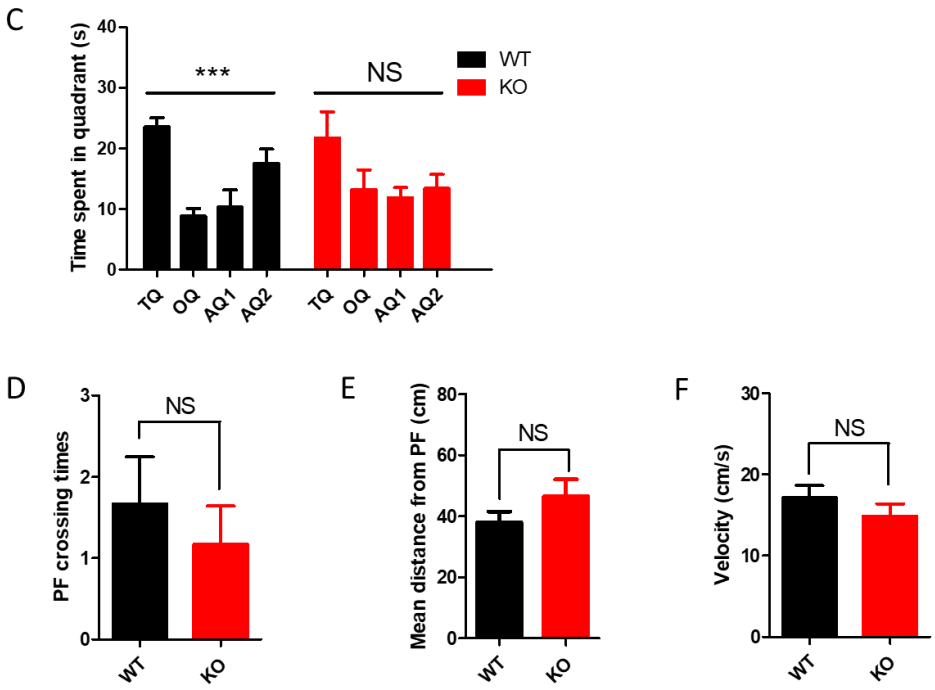

Probe test 2 at day 11

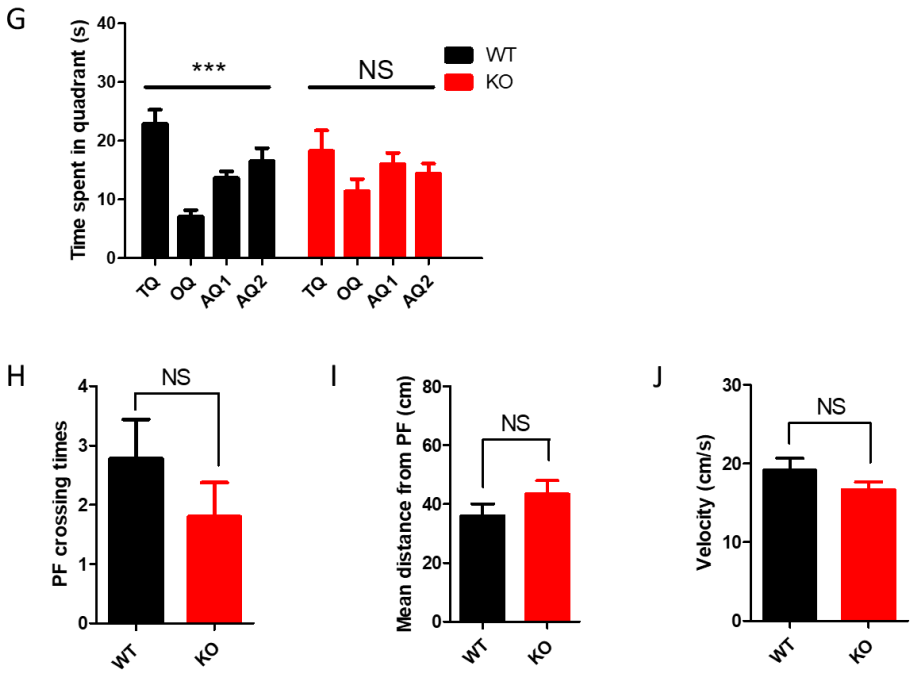

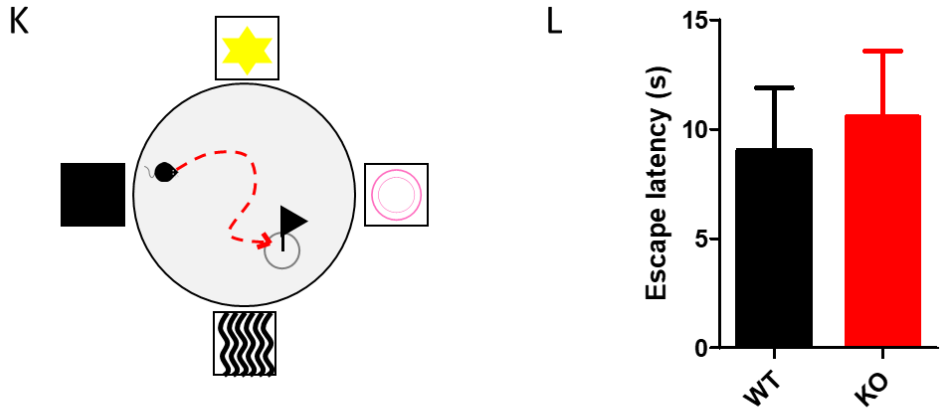
K
L
15
10
5
0
Escape latency (s)
WT
KO

Figure 7. *Vps13b* KO mice show impaired spatial learning and memory in the Morris water maze.

(A) The Morris water maze surrounded by four different spatial cues. (B) The learning curve shows escape latency during training (WT: n=9, KI: n=12; two−way ANOVA, genotype x time, $F_{8,152}$=2.69, **p < 0.001, effect of genotype, $F_{1,152}$=4.06, p=0.0582, effect of time, $F_{8,152}$=4.10, ***p < 0.0001). (C) Time spent in each quadrant in Probe test 1 at day 7 (WT: n=9; KO: n=12; one way−ANOVA of WT, ***p < 0.0001, Bonferroni's multiple comparison test, TQ vs OQ, ***p < 0.0001; one way−ANOVA of KO, NS p=0.1056, Bonferroni's multiple comparison test, TQ vs OQ, NS: not significant). (D) The number of platform crossings in probe test 1 at day 7 (WT: 1.667±0.5774, n=9; KO: 1.167±0.4741, n=12; unpaired *t*−test, p=0.5080). (E) Mean distance from platform at day 7 (WT: 38.04±3.514, n=9; KO: 46.54±5.588, n=12; unpaired *t*−test, p=0.2498). (F) Mean velocity at day 7(WT: 17.13±1.493, n=9; KO: 14.86±1.522, n=12; unpaired *t*−test, p=0.3110). (G) Time spent in each quadrant in Probe test 2 at day 11 (WT: n=9, one−way ANOVA of WT, ***p < 0.0001, Bonferroni's multiple comparison test, TQ vs OQ, ***p < 0.0001; KO: n=10, one−way ANOVA of KO, NS p=0.2422,

Bonferroni's multiple comparison test, TQ vs OQ, NS: not significant).

(H) The number of platform crossings at day 11 (WT: 2.778±0.6620, n=9; KO: 1.800±0.5735, n=10; unpaired *t*-test, p=0.2775). **(I)** Mean distance from platform at day 11 (WT: 36.06±4.047, n=9; KO: 43.37±4.581, n=10; unpaired *t*-test, p=0.2523). **(J)** Mean velocity at day 7(WT: 19.11±1.568, n=9; KO: 16.65±1.001, n=10; unpaired *t*-test, p=0.1932). TQ: target, OQ: opposite, AQ1: right, AQ2: left quadrant. **(K)** The Morris water maze with visual platform. **(L)** The escape latency for visual platform task (WT: 9.039±2.847; n=9, KO: 10.56±3.004, n=12; unpaired *t*-test, p=0.7250). All data shown are mean±SEM.

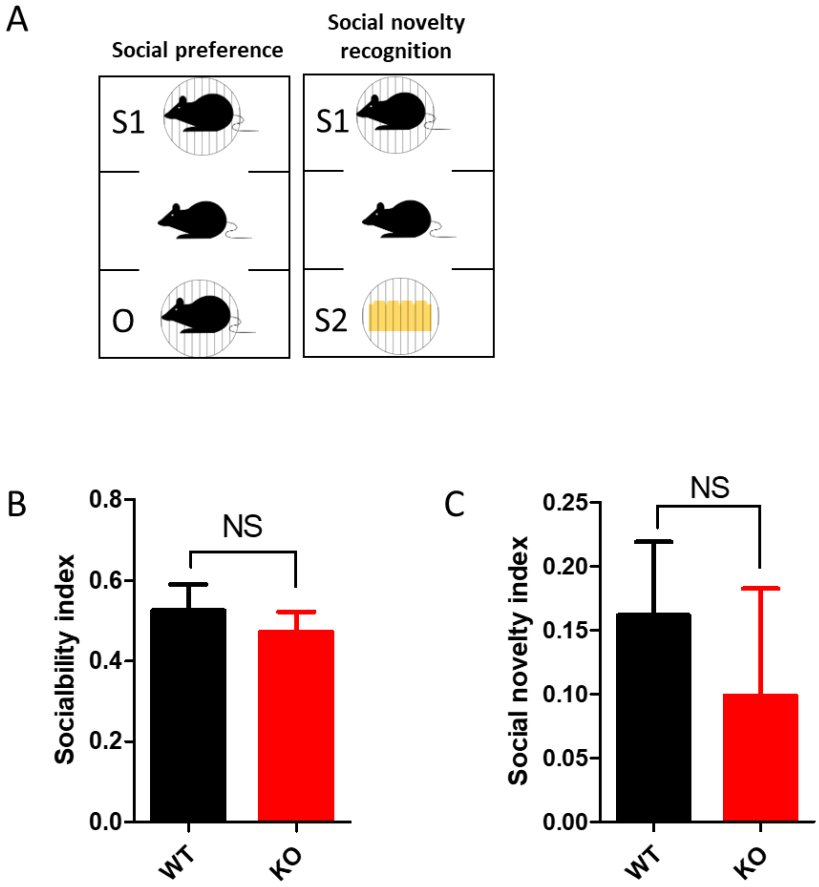
A
Social preference
Social novelty recognition
S1
S1
O
S2
B
Socialbility index
0.8
0.6
0.4
0.2
0.0
NS
WT
KO
C
Social novelty index
0.25
0.20
0.15
0.10
0.05
0.00
NS
WT
KO

Figure 8. *Vps13b* KO mice show normal social interaction in three-chamber assays.

(A) Three-chamber test. (B) Sociability index was calculated by [Time spent interacting with object − stranger1] / [Time spent interacting with object + stranger1] (WT: 0.5250±0.06499, n=9; KO: 0.4713±0.05070, n=12; unpaired *t*-test, NS p=0.5158). (C) Sociability novelty index was calculated by [Time spent interacting with stranger1 − stranger2] / [Time spent interacting with stranger1 + stranger2] (WT: 0.1616±0.05751, n=9; KO: 0.09870±0.08370, n=12; unpaired *t*-test, NS p=0.5707). NS, not significant. All data shown are mean±SEM.

Behavior	*Vps13b* KO mice phenotypes
Open field test	Hypoactivity
Elevated zero maze	No difference compared to WT
Light dark box test	Tendency to show more anxiety
Y-maze	Normal working memory, but tendency to be hypoactive
Contextual fear conditioning	No difference compared to WT
Morris water maze (hidden platform)	Impairment in spatial learning and memory
Morris water maze (visual platform)	Normal vision
Three-chamber test	No difference compared to WT

WT : wild-type

Table 2. Summary table of *Vps13b* KO mice phenotypes.

Discussion

This is the first report showing behavioral phenotypes of *Vps13b* KO mice. These mice showed normal anxiety-like behavior in various tasks, including open field test and elevated zero maze test (Fig. 3, 4B). Although *Vps13b* KO mice displayed a tendency of anxiety in the light dark box test, there was no overall difference in anxiety-like behavior between WT and KO groups (Fig. 4D). *Vps13b* KO mice showed hypoactivity in the open field test (Fig. 3C, 3D, 3E). This result raises the possibility that there may be a correlation between *VPS13B* and motor related genes and *VPS13B* and motor-corresponding brain regions, like cerebellar or basal ganglia (Lalonde et al., 2007). Hypoactivity may represent a motor clumsiness behavior, which is one of the CS phenotypes. However, in order to evaluate the motor coordination more precisely, other performance tests, like a rotarod task, should be conducted (Shiotsuki et al., 2010). *Vps13b* KO mice showed normal working memory and fear memory (Fig. 5, 6), but spatial memory deficit, which was not due to visual impairment, in the Morris water maze task (Fig. 7). It seemed that impaired spatial memory in *Vps13b* KO mice reflected learning disability which was seen in general CS patients (Duplomb et al., 2014). *Vps13b* KO mice showed comparable sociability index and

social novelty index, compared to WT mice (Fig. 8).

Spatial learning and memory is highly linked to excitatory synaptic transmission, which is mediated by glutamate receptors in the hippocampal brain regions, like dentate gyrus, CA1 and CA3 regions (Morris et al., 1990; Tombaugh et al., 2002; Foster et al., 1999). Thus, further experiments will be necessary, for instance electrophysiology, to determine whether learning and memory deficit in *Vps13b* KO mice is affected by any dysfunctions of NMDA or AMPA receptors and NMDA receptor-dependent synaptic plasticity (Tsien et al., 1996; Schmitt et al., 2004; Reisel et al., 2002; Andrasfalvy et al., 2003).

It is still largely unknown how VPS13B affects CS in terms of molecular and cellular basis. Neuronal autophagy is a lysosome-dependent degradative and recycling process that is essential for neuronal homeostasis (Lee et al., 2013). Its dysfunction contributes to neurodegenerative and neurodevelopmental disorders (Lee et al., 2013). Muñoz-Braceras et al. revealed that VPS13A regulates autophagy, and suggested that VPS13C, which shares similar amino acid identity with VPS13A, may be also implicated in autophagy (Muñoz-Braceras et al., 2015). Moreover, VPS13B is a peripheral membrane protein that performs an important function in intercellular protein transport and vesicle-mediated sorting, and therefore it is

responsible for Golgi apparatus integrity (Seifert et al., 2011). Since trans-Golgi releases lysosome which fuses with another organelles to undergo autophagy process, there may be relationship between VPS13B and autophagy. Additional study on induced neuronal cell derived from CS patient's induced pluripotent stem cell revealed that an autophagy defect was observed in CS patient (data not shown).

CS patients exhibit not only intellectual disability, but also many other symptoms, including microcephaly, myopia, neutropenia, abnormal fat storage, and distinctive facial malformation (El Chehadeh et al., 2010). Therefore, these phenotypes could be investigated anatomically and histologically. Moreover, future research should also include screening for specific pathways or compounds that restore defective features seen in *Vps13b* KO mice.

In conclusion, my findings demonstrate a *Vps13b* mutation appears to lead to partial cognitive dysfunction and motor abnormality.

References

Seifert, W., Kühnisch, J., Maritzen, T., Lommatzsch, S., Hennies, H.C., Bachmann, S., Horn, D., Haucke, V. (2015). Cohen syndrome-associated protein COH1 physically and functionally interacts with the small GTPase RAB6 at the Golgi complex and directs neurite outgrowth. The Journal of biological chemistry *290*, 3349-3358.

Seifert, W., Kühnisch, J., Maritzen, T., Horn, D., Haucke, V., Hennies, H.C. (2011). Cohen syndrome-associated protein, COH1, is a novel, giant Golgi matrix protein required for Golgi integrity. The Journal of biological chemistry *286*, 37665-37675.

Kolehmainen, J., Black, G.C., Saarinen, A., Chandler, K., Clayton-Smith, J., Träskelin, A.L., Perveen, R., Kivitie-Kallio, S., Norio, R., Warburg, M., Fryns, J.P., de la Chapelle, A., Lehesjoki, AE. (2003). Cohen syndrome is caused by mutations in a novel gene, COH1, encoding a transmembrane protein with a presumed role in vesicle-mediated sorting and intracellular protein transport. American Journal of Human Genetics *72*, 1359-1369.

Velayos-Baeza, A., Vettori, A., Copley, R.R., Dobson-Stone, C., Monaco, A.P. (2004). Analysis of the human VPS13 gene family. Genomics *84*, 536-549.

Limoge, F., Faivre, L., Gautier, T., Petit, J.M., Gautier, E., Masson, D., Jego, G., El Chehadeh-Djebbar, S., Marle, N., Carmignac, V., Deckert, V., Brindisi, M.C., Edery, P., Ghoumid, J., Blair, E., Lagrost, L., Thauvin-Robinet, C., Duplomb, L. (2015). Insulin response dysregulation explains abnormal fat storage and increased risk of diabetes mellitus type 2 in Cohen Syndrome. Human molecular genetics *24*, 6603-6613.

Duplomb, L., Duvet, S., Picot, D., Jego, G., El Chehadeh-Djebbar, S., Marle, N., Gigot, N., Aral, B., Carmignac, V., Thevenon, J., Lopez, E., Rivière, J.B., Klein, A., Philippe, C., Droin, N., Blair, E., Girodon, F., Donadieu, J., Bellanné-Chantelot, C., Delva, L., Michalski, J.C., Solary, E., Faivre, L., Foulquier, F., Thauvin-Robinet, C. (2014). Cohen syndrome is associated with major glycosylation defects. Human molecular genetics *23*, 2391-2399.

El Chehadeh, S., Aral, B., Gigot, N., Thauvin-Robinet, C., Donzel, A., Delrue, M.A., Lacombe, D., David, A., Burglen, L.,

Philip, N., et al. (2010). Search for the best indicators for the presence of a VPS13B gene mutation and confirmation of diagnostic criteria in a series of 34 patients genotyped for suspected Cohen syndrome, J. Med. Genet. *47*, 549-553.

El Chehadeh-Djebbar, S., Blair, E., Holder-Espinasse, M., Moncla, A., Frances, A.M., Rio, M., Debray, F.G., Rump, P., Masurel-Paulet, A., Gigot, N., et al. (2012). Changing facial phenotype in Cohen syndrome: towards clues for an earlier diagnosis. Eur. J. Hum. Genet. *21*, 736-742.

Morris, R.G., Schenk, F., Tweedie, F., Jarrard, L.E. (1990). Ibotenate Lesions of Hippocampus and/or Subiculum: Dissociating Components of Allocentric Spatial Learning. Eur J Neurosci. *2*, 1016-1028.

Tombaugh, G.C., Rowe, W.B., Chow, A.R., Michael, T.H., Rose, G.M. (2002). Theta-frequency synaptic potentiation in CA1 in vitro distinguishes cognitively impaired from unimpaired aged Fischer 344 rats. J. Neurosci. *22*, 9932-9940.

Foster, T.C. (1999). Involvement of hippocampal synaptic plasticity in age-related memory decline. Brain Res Brain Res Rev. *30*, 236-

249.

Andrasfalvy, B. K., Smith, M. A., Borchardt, T., Sprengel, R. & Magee, J. C. (2003). Impaired regulation of synaptic strength in hippocampal neurons from GluR1-deficient mice. J Physiol. *552*, 35-45.

Reisel, D., Bannerman, D.M., Schmitt, W.B., Deacon, R.M., Flint, J., Borchardt, T., Seeburg, P.H., Rawlins, J.N. (2002). Spatial memory dissociations in mice lacking GluR1. Nat Neurosci. *5*, 868-873.

Schmitt, W.B., Deacon, R.M., Reisel, D., Sprengel, R., Seeburg, P.H., Rawlins, J.N., Bannerman, D.M. (2004). Spatial reference memory in GluR-A-deficient mice using a novel hippocampal-dependent paddling pool escape task. Hippocampus *14*, 216-223.

Murphy, C.M., Wilson, C.E., Robertson, D.M., Ecker, C., Daly, E.M., Hammond, N., Galanopoulos, A., Dud, I., Murphy, D.G., McAlonan, G.M. (2016). Autism spectrum disorder in adults: diagnosis, management, and health services development. Neuropsychiatr Dis Treat. *12*, 1669-1686.

Seifert, W., Holder-Espinasse, M., Kühnisch, J., Kahrizi, K., Tzschach, A., Garshasbi, M., Najmabadi, H., Walter Kuss, A., Kress, W., Laureys, G., Loeys, B., Brilstra, E., Mancini, G.M., Dollfus, H., Dahan, K., Apse, K., Hennies, H.C., Horn, D. (2009). Expanded mutational spectrum in Cohen syndrome, tissue expression, and transcript variants of COH1. Hum Mutat. *30*, 404-420.

Muñoz-Braceras, S., Calvo, R., Escalante, R. (2015). TipC and the chorea-acanthocytosis protein VPS13A regulate autophagy in Dictyostelium and human HeLa cells. Autophagy *11*, 918–927.

Lee, K.M., Hwang, S.K., Lee, J.A. (2013). Neuronal autophagy and neurodevelopmental disorders. Exp Neurobiol. *22*, 133-142.

Houtkooper, R.H., Argmann, C., Houten, S.M., Cantó, C., Jeninga, E.H., Andreux, P.A., Thomas, C., Doenlen, R., Schoonjans, K., Auwerx, J. (2011). The metabolic footprint of aging in mice. Sci Rep. *1*, 134.

Kaczmarczyk, L., Jackson, W.S. (2015). Astonishing advances in mouse genetic tools for biomedical research. Swiss Med Wkly. *145*.

Sakimoto, H., Nakamura, M., Nagata, O., Yokoyama, I., Sano, A. (2016). Phenotypic abnormalities in a chorea-acanthocytosis mouse model are modulated by strain background. Biochem Biophys Res Commun. *472*, 118-124.

Vonk, J.J., Yeshaw, W.M., Pinto, F., Faber, A.I., Lahaye, L.L., Kanon, B., Zwaag, M. V., Velayos-Baeza, A., Freire, R,. IJzendoorn, S. C., Grzeschik, N. A., Sibon, O. C. (2017). Drosophila Vps13 Is Required for Protein Homeostasis in the Brain. PLoS One. *12*, e0170106.

Cho, S.W., Kim, S., Kim, J.M., Kim, J.S. (2013). Targeted genome engineering in human cells with the Cas9 RNA-guided endonuclease. Nat Biotechnol. *3*, 230-232.

Lalonde, R., Strazielle, C. (2007). Brain regions and genes affecting postural control. Progress in Neurobiology *81*, 45–60.

Jinek, M., Chylinski, K., Fonfara, I., Hauer, M., Doudna, J.A., Charpentier, E. (2012). A programmable dual-RNA-guided DNA endonuclease in adaptive bacterial immunity. Science. *337*, 816-821.

Knight, E. M., Ruiz, H. H., Kim, S. H., Harte, J. C., Hsieh, W., Glabe,

C., Klein, W. L., Attie, A. D., Buettner, C., Ehrlich, M. E., Gandy, S. (2016). Unexpected partial correction of metabolic and behavioral phenotypes of Alzheimer's APP/PSEN1 mice by gene targeting of diabetes/Alzheimer's-related Sorcs1. Acta Neuropathol Commun. *4*, 16.

Balikova, I., Lehesjoki, A.E., de Ravel, T.J., Thienpont, B., Chandler, K.E., Clayton-Smith, J., Träskelin, A.L., Fryns, J.P., Vermeesch, J.R. (2009). Deletions in the VPS13B (COH1) gene as a cause of Cohen syndrome. Hum Mutat. *30*, E845-54.

Rampoldi, L., et al. (2001). A conserved sorting-associated protein is mutant in chorea-acanthocytosis. Nat Genet. *28*, 119-20.

Ueno, S., Maruki, Y., Nakamura, M., Tomemori, Y., Kamae, K., Tanabe, H., Yamashita, Y., Matsuda, S., Kaneko, S., Sano, A. (2001). The gene encoding a newly discovered protein, chorein, is mutated in chorea-acanthocytosis. Nat Genet. *28*, 121-2.

Lesage, S., et al. (2016). Loss of VPS13C Function in Autosomal-Recessive Parkinsonism Causes Mitochondrial Dysfunction and Increases PINK1/Parkin-Dependent Mitophagy. Am J Hum Genet. *98*,

500-513.

Yu, T.W., et al. (2013). Using whole-exome sequencing to identify inherited causes of autism. Neuron *77*, 259-273.

Tsien, J.Z., Huerta, P.T., Tonegawa, S. (1996). The essential role of hippocampal CA1 NMDA receptor-dependent synaptic plasticity in spatial memory. Cell *87*, 1327-1338.

Shiotsuki, H., Yoshimi, K., Shimo, Y., Funayama, M., Takamatsu, Y., Ikeda, K., Takahashi, R., Kitazawa, S., Hattori, N. (2010). A rotarod test for evaluation of motor skill learning. J Neurosci Methods. *189*, 180-185.

국 문 초 록

VPS13B 단백질에 대한 연구는 주로 골지체와 같은 세포 소기관과 관련된 기능에 초점이 맞추어져 이루어졌다. 또한 여러 환자 연구에 따르면 코헨 신드롬 환자에게서 *VPS13B* 유전자 돌연변이가 일어난다고 보고된 바 있고, 최근에는 자폐 스펙트럼 장애를 가진 환자에게서도 변이가 발견되었다는 보고가 있다. 유전자에 대한 연구는 특정 유전자 변이를 지닌 환자처럼 인간 모델에서 이루어지는 것이 가장 이상적이지만 복합적인 윤리 문제 때문에 현실적으로 이루어 지기에는 많은 어려움이 따른다. 따라서 많은 연구에서는 인간 모델보다는 동물 모델을 주로 사용하고 있다. 그 중에서도 인간과 유사한 특징을 지닌 마우스 모델을 이용하여 유전자 연구가 행해지고 있다.

본 연구는 처음으로 *Vps13b* 유전자의 엑손 2 일부가 삭제된 유전자 적중 마우스를 이용하여 여러 행동학적 표현형을 관찰하고자 하였고 질병에 대한 마우스 모델로서의 가능성을 확인하고자 하였다. 결과적으로 *Vps13b* 유전자 적중 마우스는 야생형 마우스와 비교하였을 때 불안행동, 작업기억, 시각, 해마 의존적 공포 기억, 사회성 행동 양상이 모두 정상인 것을 나타났다. 모리스 워터 메이즈을 통해서는 공간적 학습·기억이 결핍된 것을 확인하였고 불안 유사 행동을 나타내는 행동 실험 중 하나인 오픈 필드 테스트에서는 확연히 저활동성을 보였다. 이는 *Vps13b* 유전자를 적중시켰을 경우, 코헨 신드롬이나 자폐 장애 환자에게서 나타나는 증상인 둔한 움직임과 인지

기능이 일부적으로 상실되는 것을 통해 마우스 질병 모델로서의 가능성을 보여주었다.

주요어 : 코헨 신드롬, *Vps13b* 유전자 적중 마우스, 행동 연구, 저활동성, 공간적 학습 및 기억

학 번 : 2016-20393